Optik - International Journal for Light and Electron Optics 241 (2021) 166949

Contents lists available at ScienceDirect

Optik

journal homepage: www.elsevier.com/locate/ijleo

Original research article

Design and synthesis of highly conjugated Electronic Phenanthrolines Derivatives for remarkable NLO properties and DFT analysis

F.A. Sahki [a], A. Bouraiou [a], S. Taboukhat [b], L. Messaadia [c], S. Bouacida [a,d], V. Figa [e], K. Bouchouit [f,*], B. Sahraoui [b,*]

[a] Unité de Recherche de Chimie de l'Environnement, et Moléculaire Structurale, CHEMS, Université Frères Mentouri, Constantine 25000, Algeria
[b] Laboratory MOLTECH-Anjou, CNRS UMR 6200, University of Angers, 2 Bd Lavoisier, 49045 Angers CEDEX, France
[c] Laboratoire Énergétique Appliquée et Matériaux (LEAM), Université de Jijel, Ouled Aissa, Jijel, Algeria
[d] Département Sciences de la Matière, Université Oum El Bouaghi, 04000 Oum El Bouaghi, Algeria
[e] Euro-Mediterranean Institute of Science and Technology (IEMEST), via Michele Miraglia 20, 90100 Palermo, Italy
[f] Ecole Normal Supérieure de Constantine, Ville Universitaire, Constantine, Algerie

ARTICLE INFO

Keywords:
Phenanthrolines
Structural features
Nonlinear Optics
THG
Hyperpolarizability
DFT
All optical switching

ABSTRACT

The non-linear optical technology is gaining huge attention to the thermal and mechanical stability, electrical property, and modulate signal flexibility that could be used in uprising opto-electronics devices based on powerful laser technologies such as all optical switches, light-emitting diodes, data storage and optical communication systems. In this paper, selected three phenanthrolines derivatives [2-phenyl-1*H*-phenanthro[9,10-*d*]imidazole (**1**), 2-(4-nitrophenyl)-1*H*-phenanthro[9,10-*d*]imidazole(**2**),2-(4-methoxyphenyl)-1*H* phenanthro[9,10-*d*]imidazole (**3**)] were synthesized and characterized using UV, FT-IR and ^{1}H NMR. Cubic nonlinear optical properties susceptibility ($\chi^{<3>}_{THG}$) were analyzed and evaluated using the third harmonic generation technique on thin films at 1064 nm. The investigation study is completed by a theoretical calculation in which the different quantum chemical parameters like frontier molecular orbital analysis, energy gap, dipole moment, average polarizability, and first second hyperpolarizability were analyzed using Density Functional Theory (DFT). The non-linear optical behavior of the selected three phenanthrolines derivatives is confirmed through the obtained high THG efficiency. Moreover, a significant correlation between the molecular structures and the optoelectronic properties is demonstrated.

1. Introduction

The design and synthesis of new organic molecules with multidisciplinary applications, such as optic, physical-chemistry, pharmacology, medicine, and other fields have always attracted the attention of the community of scientists. The development of organic NLO properties compounds has been facilitated by the organic chemist's extensive knowledge of the optical properties. [1–10]. The conjugated π electron system especially is preferred to bind to the electro-donor and electro-acceptor groups. Phenanthrolines derivatives molecules with a π conjugated system present an ideal NLO system because of his large charge transfer through substituent

* Corresponding authors.
E-mail addresses: karim.bouchouit@laposte.fr (K. Bouchouit), bouchta.sahraoui@univ-angers.fr (B. Sahraoui).

https://doi.org/10.1016/j.ijleo.2021.166949
Received 10 July 2020; Received in revised form 2 March 2021; Accepted 13 April 2021
Available online 1 May 2021

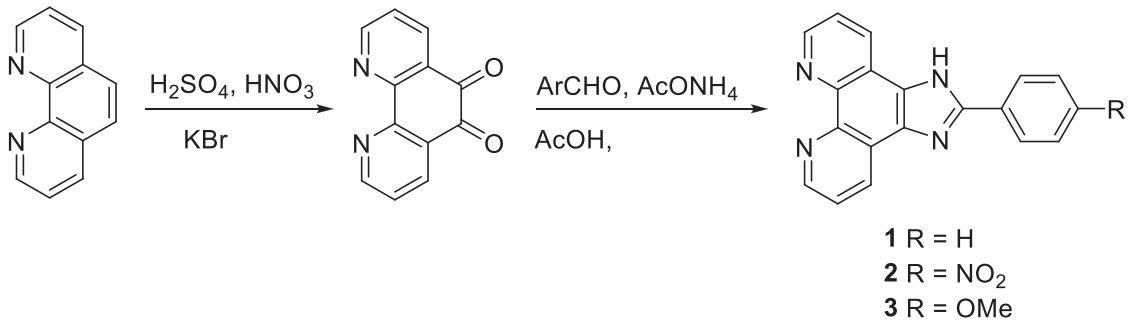

Scheme 1. Synthetic pathway.

groups on the aromatic rings [11–16]. This class of organo-electronics molecules exhibits a potential applications in biochemistry [17–20], photochemistry [21,22], nonlinear optics [23–26], electroluminescence [27,28] and many other advantageous properties, etc. Due to the highs electronics potentials of these heteroaromatics rings and their derivatives.

Phenanthrolines derivatives are polycyclic organic ligands versatile moieties which have found use in many applications [29–32] due to their interesting properties. Usually these molecules are used in the complexation and coordination chemistry [33–35]. Also, these molecules present an important place in the design of organo-compounds with highs nonlinearities.

2-Arylimidazo[4,5-*f*]-1,10-phenanthroline is an attractive ligand and a number of compounds based on this nucleus with different structural and electronic properties have been designed and synthesized [36,37]. The possibility of incorporating an electron-withdrawing or electron-donating groups at the benzaldehyde-precursor of 2-arylimidazo[4,5-*f*]-1,10- phenanthroline have a better effect on their HOMO and LUMO energies and then therefore on the photo-physical properties [38,39]. A considerable number of metal complexes of this organo-electronics ligand such as those of Eu(II), La(III) and Ru(II) have been described and have shown interesting photophysical properties [40–42].

Following to our later studies which are focused on the origin of the nonlinear response and the correlation between the chemical structure and the nonlinear properties [43–46]. Herein, we present the details of three phenanthroline derivatives: the synthesis, characterization, optical, and NLO properties. The cubic nonlinear optical properties of phenanthrolines derivatives were evaluated using the third harmonic generation technique on thin films at 1064 nm. Few important parameters like frontier molecular orbital analysis, first and second hyperpolarizability, electronic transitions, and molecular electrostatic potential (MESP) analysis have been performed to explore the optoelectronic, photophysical and photovoltaic properties of designed and reference molecule.

2. Experimental details

2.1. General considerations

All reagents were used without further purification and were purchased as analysis grade. ^{1}H NMR spectra were recorded on Brüker Avance DPX250 spectrometers. The melting points of the synthesized compounds were determined using an Electrothermal IA 9100 digital melting point apparatus. The UV spectra of the three phenanthrolines derivatives were analyzed on UV/VIS Spectrophotometer Optizen 1220; Infrared (IR) samples were prepared as KBr pellets and their spectra collected in the range 400–4000 cm-1 on Shimadzu FT/IR-8201 PC spectrophotometer.

2.2. Synthesis

All reagents and solvents used in this study were purchased from Sigma Aldrich, and used without further purification.

The synthetic pathways of the studied ligands 1–3 are illustrated in Scheme 1. According to a modified literature procedure [47], 1, 10-Phenanthroline-5,6-dione was prepared. These molecules were synthesized according to the literature procedure [48].

2.2.1. Synthesis of 2-aryl-1H-phenanthro[9,10-d]imidazole derivatives

1,10-Phenanthroline-5,6-dione (100 mg, 0.48 mmol) which was prepared in accordance with established methods [47] was dissolved in glacial acetic acid (5 ml). Aromatic aldehyde (0.48 mmol) and ammonium acetate (14.4 mmol) were added. The mixture was heated at reflux for 10 h. After the reaction was complete, the reaction solution was cooled to room temperature, diluted with water then neutralized with aqueous ammonia and pH was adjusted to 8–9. The resulting precipitate was filtered and dried.

Table 1
The values of third order nonlinear optical susceptibility ($\chi^{<3>}_{THG}$) and the of absorption coefficients of phenanthroline derivatives thin films obtained from THG experiment.

Simple	d (Å)	$\chi^{<3>}_{THG}$. 10^{22} [m^2/V^2]	α [10^3 cm^{-1}] at 355 nm
1	2200	46.27	4.27
2	2000	105.32	27
3	2100	60.03	4.61
Silica	–	2	–

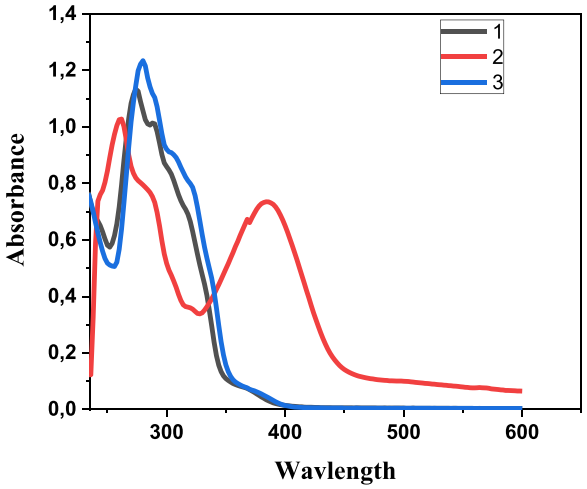

Fig. 1. Absorption spectra of the three studied compounds dissolved in solutions.

2.2.2. 2-phenyl-1H-phenanthro[9,10-d]imidazole (1)

Yield 95%; Yellow solid; mp. > 300 °C (literature = 390–392 °C [49]); IR (KBr) υ 3429, 1635, 1554, 1411, 1149, 802, 690; ^{1}H NMR (250 MHz, DMSO-d_6): δ: 13.35 (s, 1H), 9.05 (dd, J = 4.2 Hz, J = 1.4 Hz, 2H), 8.93 (dd, J = 7.9 Hz, J = 1.3 Hz, 2H), 8.30 (d, J = 8.0 Hz, 2H), 7.85–7.82 (m, 2H), 7.63 (t, J = 7.9, 2H), 7.52 (t, J = 7.1 Hz, 1H); UV–Vis (MeOH, λ/nm): 224, 274.

2.2.3. 2-(4-nitrophenyl)-1H-phenanthro[9,10-d]imidazole (2)

Yield 97%; Yellow solid; mp. > 300 °C (literature = 339 °C[50]); IR (KBr) υ, 1600, 1558, 1515, 1415, 1342, 1149, 856, 806; ^{1}H NMR (250 MHz, DMSO-d_6): δ: 9.20–9.17 (m, 2H), 9.10–9.07 (m, 1H), 8.74–7.72 (m, 1H), 7.84–7.79 (m, 4H), 7.56–7.50 (m, 3 H) ppm; UV–Vis (MeOH, λ/nm): 262, 384.

2.2.4. 2-(4-methoxyphenyl)-1H-phenanthro[9,10-d]imidazole (3)

Yield 90%; orange solid; mp. > 300 °C (literature >300 °C [51]); IR (KBr) υ 3425, 1612, 1562, 1481, 1438, 1253, 1176, 1026, 952, 802, 732; ^{1}H NMR (300 MHz, DMSO-d_6): δ 12.99 (s, 1H), 9.00 (d, J = 4.3 Hz, 1H), 8.90 (d, J = 8.0 Hz, 2 H), 8.22 (d, J = 7.9 Hz, 2 H), 7.86–7.78 (m, 2H), 7.20 (d, J = 8 Hz, 2 H), 3.85 (s, 3H); UV–Vis (MeOH, λ/nm): 226, 280.

2.3. Thin film preparation and optical absorption measurements

Thin films of the three phenanthrolines derivatives compounds 1–3 were prepared from DMSO (Dimethyl sulfoxide) solution with a concentration of 10 mg/ml. The homogeneous spreading out of the prepared solutions were deposited on cleaned glass substrates by using spin-coater at 1200 rpm. To eliminate any remaining solvent obtained thin films were kept at 60 °C for 4 h in the oven. Thickness details of elaborated thin films was measured by using profilometer (Dektak 6M) they are around 2000 A. The values of thickness and third order nonlinear optical susceptibility ($\chi^{<3>}_{THG}$) are reported in Table 1.

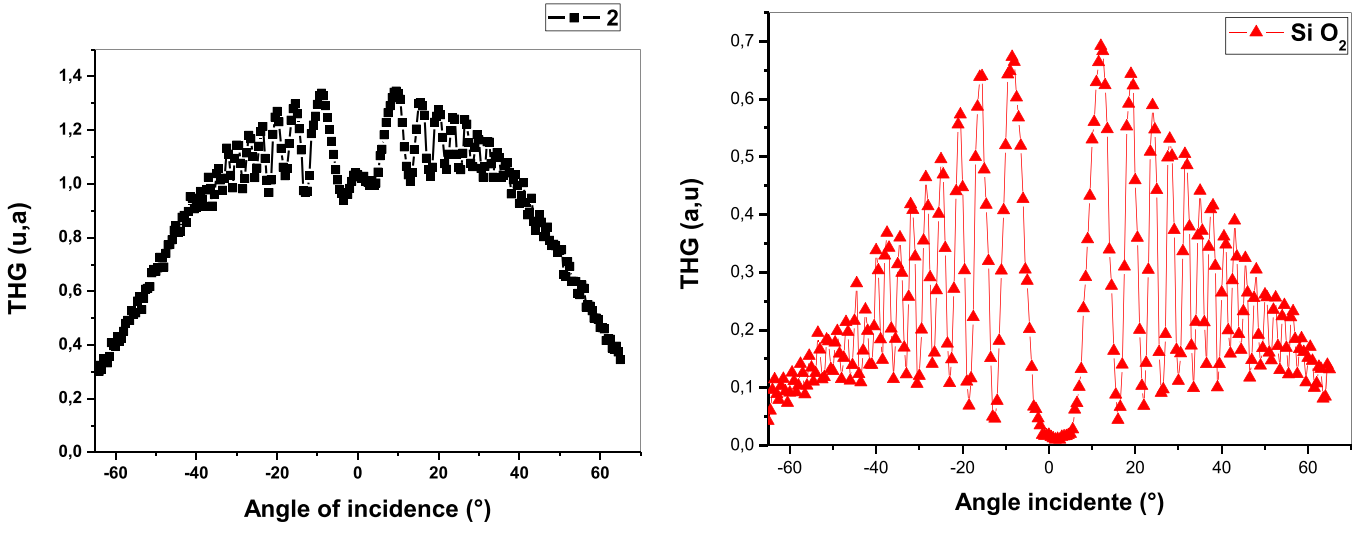

Fig. 2. THG response of silica glass and compound 2 thin film in p-polarization.

Table 2
Calculated first and second order hyperpolarizabilities components (β, γ) using DFT at 6-31G(d, p).

Components	1	2	3
β_{xxx}	0.179431	0.129274	0.431312
β_{xxy}	-0.923705	0.199755	-0.257877
β_{xyy}	-0.497066	-0.627543	0.485066
β_{yyy}	-0.148487	-0.168091	-0.84372
β_{xxz}	0.638572	-0.213179	0.136696
β_{xyz}	0.125859	-0.524198	-0.454971
β_{yyz}	0.186262	-0.100062	-0.354395
β_{xzz}	0.208151	0.157046	-0.314417
β_{yzz}	-0.147458	-0.149848	0.277512
β_{zzz}	-0.407619	0.156483	0.176857
β_{tot} (10^{-30} esu)	11.41	106.2	8.113
γ_{xxxx}	326.45	1880.28	10.7972
γ_{yyyy}	43.8833	44.8105	38.7533
γ_{zzzz}	0.240564	0.238467	235.817
γ_{xxyy}	18.669	65.5431	15.1742
γ_{xxzz}	2.36625	5.37974	44.4447
γ_{yyzz}	2.12996	2.19414	52.7914
γ_{tot}(10^{-36}esu)	83.380	414.312	102.037

2.4. Nonlinear optical measurements

By using a well-known Maker fringe setup [52,53], the third harmonic NLO properties measurements were carried out. Samples were rotated from − 70° to + 70° and intensity of generated harmonics as a function of incident angle was measured in p-polarization. The laser used for these measurements has the following characteristics; the fundamental wavelength beam was 1064 nm, frequency of 10 Hz, 30 ps pulse duration and energy of 60 μJ.

2.5. Geometrical structure analysis

The geometrical structures of the three phenanthrolines derivatives compounds 1–3 were optimized and analyzed with B3LYP/6-31G (p, d) level using Gaussian 09 software programs [54]. And the Gauss-view molecular visualization package [55]. Density functional theory (DFT) was used in this work, with the combination of the Becke's three-parameter hybrid exchange-correlation functional of Lee, Yang, and Parr (B3LYP) [56,57] to optimize and to calculate a few quantum chemical parameters, such as: Dipole moment, polarizability, the first (β), second hyperpolarizabilities (γ), energy gap (HOMO-LUMO), and molecular reactivity.

3. Results and discussion

3.1. UV–visible spectra

The absorption UV–vis spectra of all compounds are dissolved in methanol solutions are characterized by the presence of the intense absorption bands between 260 and 275 nm, which are assigned to π → π* transitions. Also, a less intense absorption band at 385 nm, which is assigned to n → π* transition in the lower energy part of the spectra is observed for compound 2. Moreover we can notice that the three phenanthroline derivatives compound present high transparency at the wavelength of more than 500 nm. Moreover, from absorption spectra (Fig. 1) one observes that at wavelengths generated by third harmonics (THG), the absorbance is not negligible.

3.2. THG results

To extract and evaluated the third-order NLO susceptibility of the three compounds thin films. Third harmonic generation measurements have been performed on thin films at 1064 nm.

However, third-order nonlinear optical susceptibility was calculated by using the Wang model [58]:

$$\chi^{(3)} = \chi^{(3)}_{Silica}\left(\frac{2}{\pi}\right)\left(\frac{L^{coh}_{Silica}}{d}\right)\left(\frac{\frac{\alpha d}{2}}{1-exp\left(-\frac{\alpha d}{2}\right)}\right)\sqrt{\frac{I^{3\omega}}{I^{3\omega}_{Silica}}} \quad (1)$$

Table 3
Quantum chemical parameters of compounds 1–3 using B3LYP/ 6-31G (p, d).

Parameters	Compounds		
	1	2	3
Total energy (Hartree)	-950.31596434	-1154.8151046	-1064.84195166
E_{HOMO} (eV)	-5.586	-6.013	-5.356
E_{LUMO} (eV)	-1.436	-2.753	-1.271
$\Delta E_{L\text{-}H}$ (eV)	4.15	3.26	4.085

where: $\chi^{(3)}_{Silica} = 2 \cdot 10^{-22} m^2 \cdot V^{-2}$ [59], $L^{coh}_{Silica} = 6,7 \mu m$ is the coherence length of reference material, d – sample thickness and $I^{3\omega}$ and $I^{3\omega}_{Silica}$ are THG intensities of thin film and reference material, respectively.

Fig. 2 present THG intensities as a function of incident angle that is collected for compound 1. The $\chi^{(3)}$ THG susceptibilities values for compounds 1–3 were estimated and evaluated by comparing the TH signal with that SiO_2 glass material. As a reference material in THG measurements was used silica glass with thickness 1 mm. We used formula 1 for our calculations of $\chi^{(3)}$ susceptibilities. The calculated values of third order NLO susceptibility $\chi^{(3)}$ are given in Table 2. The obtained values of cubic susceptibility $\chi^{(3)}$ of the three phenanthrolines derivatives, thin films at a measurement wavelength of 1064 nm have been estimated at 4,6. 10^{-21} [m^2V^{-2}] and 10,5. 10^{-21} [m^2V^{-2}] (Table 2). These values are two order of magnitude larger than susceptibility $\chi^{(3)}$ value of silica. Also, we can observe from Table 1 that the cubic susceptibility $\chi^{(3)}$ THG of molecule 2 is more important than $\chi^{(3)}$ of compound 1 and 3, this difference is due to the difference between donor groups involving more charge transfer in this series of molecules. So that the influence of the electron-donating groups following this order NO2 > OCH3 > H. These experimental results are in good agreement with theoretical results obtained from Density Functional Theory (DFT); therefore the charge transfer in phenanthrolines derivatives 2 is greater than molecule 1 and 3.

3.2.1. *First hyperplarizability*

The present work aims to study the non-linear optical properties (NOL). Quantum electronic and optical chemical properties calculations were carried using the GAUSSIAN 09 [60]. The molecular structures were optimized and analyzed with the Density Functional Theory (DFT) at RB3LYP/6-31G (p, d) basis set. The polarizabilities and first static hyperplarizability characterize the answer of a system in an applied electric field [61], they are defined in [62,63]. The simulation parameters of GAUSSIAN 09 output are reported in atomic units and therefore the calculated values are converted into e.s.u. units (1 a.u. = 8.3693 9 10^{-33} esu.). A third rank tensor that can be described by a 3 × 3 × 3 matrix present the First hyperpolarizability. The 27 Components of the 3D matrix can be reduced to 10 components due to the Kleinman symmetry [64]. The total dipole moment μ, the average polarizability $\overline{\alpha}$, and the first static hyperpolarizability (β_0), and average second hyperplarizability (γ) frequency depended (0.043 a.u.) were computed by DFT using the following relations and the results are given in Table 2 using the x, y, z components they are defined as follows:

$$\mu = (\mu_x^2 + \mu_y^2 + \mu_z^2)^2$$

$$\overline{\alpha} = \frac{\alpha_x + \alpha_x + \alpha_x}{3}$$

$$\beta_0 = (\beta_x^2 + \beta_y^2 + \beta_z^2)^{1/2} \text{ and } \beta_x = \beta_{xxx} + \beta_{xyy} + \beta_{xzz}$$
$$\beta_y = \beta_{yyy} + \beta_{yzz} + \beta_{yxx}$$
$$\beta_z = \beta_{zzz} + \beta_{zxx} + \beta_{zyy}$$

$$\gamma = \frac{1}{5}(\gamma_{xxxx} + \gamma_{yyyy} + \gamma_{zzzz} + 2\gamma_{xxyy} + 2\gamma_{xxzz} + 2\gamma_{yyzz})$$

In order to investigate the correlation between the title compounds and Non-Linear Optical proprieties (NLO), the components of the polarizabilities, hyperpolarizabilities (β) and average polarizability $\alpha(\mathring{A}^3)$ were calculated.

The components of the first hyperpolarizability for the phenanthroline derivatives **1**, **2** and **3** are given in Table 2. As we noticed, the first hyperpolarizability of phenanthroline derivatives 1 is 1.83 times greater than those of 1 and 3. The results indicate clearly that **2** is better candidates in nonlinear optical material than **1 and 3**. It is expected that the compound **2** consist of combination with NO2 as the high electron-attractor group and increase of the first hyperpolarizability with the comparison to compound **3** where the O-CH_3 acts as donor group.

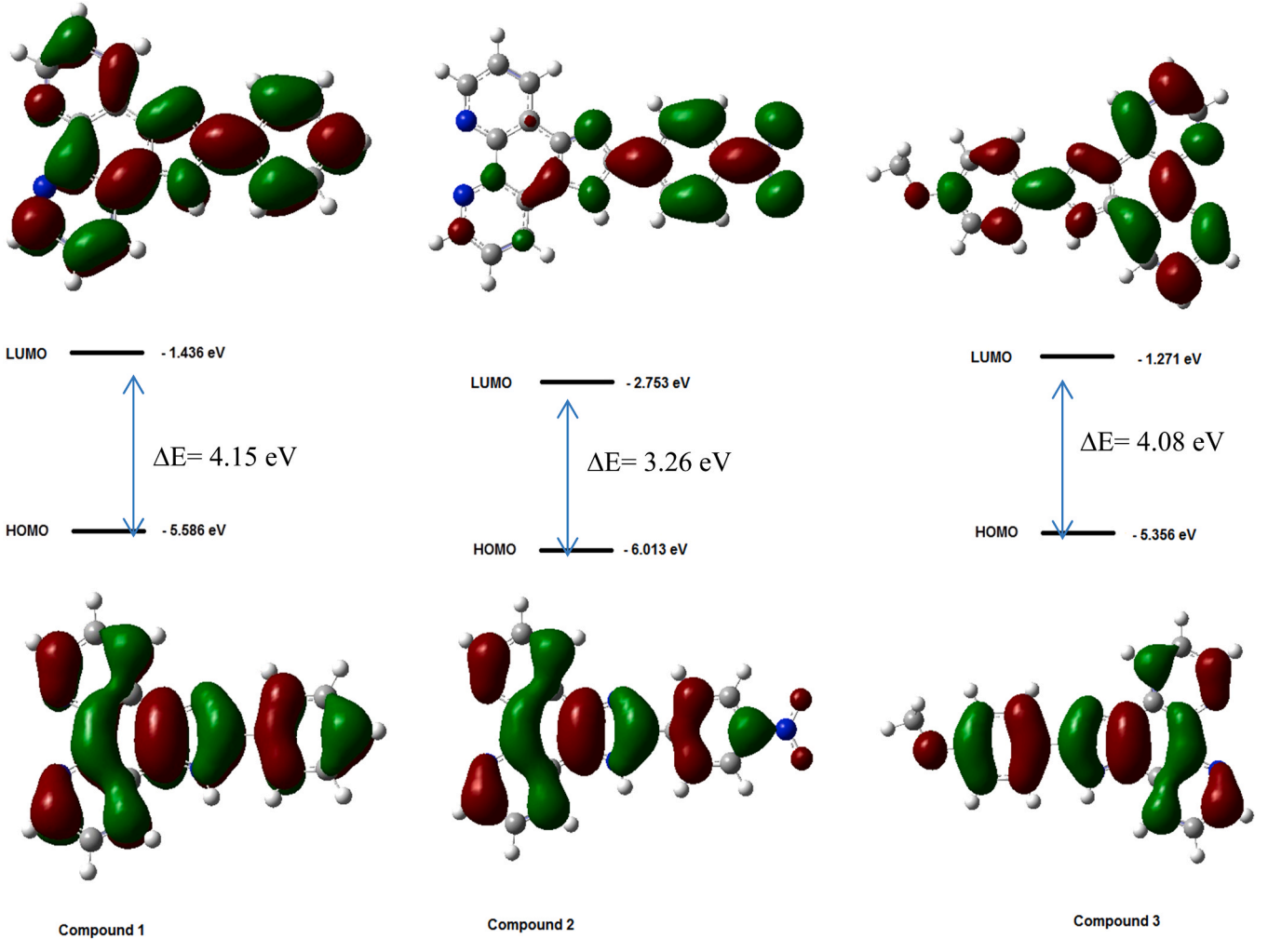

Fig. 3. Frontier Molecular Orbital plots of compounds 1–3.

Table 4

Calculated total dipole moment μ (Debye), average polarizability $\alpha(\text{Å}^3)$ of the studied compounds **1–3** using RB3LYP/6-31G (p, d).

Components	1	2	3
μ_x	4.4539	-2.6603	-5.7144
μ_y	-2.7985	0.5720	-1.7519
μ_z	0.0005	2.1639	0.0005
μ_{tot} (Debye)	5.2602	3.4766	5.9769
α_x	386.764	481.974	440.425
α_y	290.321	302.745	300.192
α_z	70.242	75.411	82.051
$\overline{\alpha}(\text{Å}^3)$	36.914	42.485	40.635
Δα (esu)	2.427×10^{-30}	3.048×10^{-30}	2.70×10^{-30}

According to the present study, the calculated values of the dipole moment μ_{tot}, average polarizability $\overline{\alpha}$, and the first static hyperpolarizability (β_0) of compound **2** are equal to 3.4582 Debye, 42.485 Å^3, and 106.27×10^{-30} esu, respectively are shown in Table 2.

The calculated values average of the polarizability $\overline{\alpha}$ and dipole moment of phenanthroline derivatives 2 is about 42.485, greater than **1** and **3**. In addition, these results indicate that phenanthroline derivatives **2** show more NLO behavior.

Therefore, as shown in Table 2, the second hyperplarizability values obtained for compounds 1,2 and 3 increase in the following sequence, compound (2) (414.312×10^{-36} esu) > compound (3) (102.037×10^{-36}esu) > compound (1) (83.380×10^{-36}esu). It is noted that the compound (2) possess higher third order nonlinear optical susceptibility than compound (3) and (1). These results are in good agreement with the experimental data. This suggested that the compound (2) is a potential candidate for NLO applications.

3.3. Frontier molecular orbitals (HOMO - LUMO) analysis

The most important molecular orbitals interaction in materials is the highest occupied molecular orbital (HOMO) and lowest unoccupied molecular orbital (LUMO).

The major role that these orbitals play is governing many chemical reactions which are responsible for the formation of many charge transfer compounds [65].

The LUMO represents the capability to obtain an electron and HOMO represents the capacity to donate an electron.

The energy gap orbitals ($\Delta E_{L\text{-}H} = E_{LUMO} - E_{HOMO}$) was calculated using the density functional theory (DFT) at B3LYP/6-31G (p, d) level, which reveals the chemical reactivity of molecules and proves the occurrence of eventual charge transfer within compounds. The optimization of the molecular geometry of the three phenanthroline derivatives in the gaseous phase was simulated in order to calculate the stability of the total energy and the energy gap between the frontier molecular orbitals. In Tables 2 and 3 there are given the results of simulation of NLO properties for the three phenanthroline derivatives together with the values of energies of HOMO and LUMO.

The frontier orbitals gap aids to characterize the chemical reactivity and kinetic stability of the compounds. A compound with a small frontier orbital gap is more polarizable, and is usually related with a best chemical reactivity, weak kinetic stability [66]. The simulated quantum chemical parameters are grouped in Table 2. we can notice that the phenanthroline derivatives **2** has lower value of energy GAP (ΔE =3.26 eV) than phenanthroline derivatives **1** and **2**. Hence, the compound **2** is more reactive, and proves the occurrence of eventual intermolecular charge transfer. The diagrams of the frontier molecular orbitals HOMO and LUMO, for the three phenanthroline derivatives were shown in Fig. 3. It can be seen from the (Fig. 3) that, the HOMO for phenanthroline derivatives **1** and **3** are delocalized almost over the whole π-conjugated system, while the LUMO, and is also delocalized over the whole compounds. In compound **2,** the HOMO is localized over the whole π-conjugated system, but he LUMO is mainly located over the $C_6H_5NO_2$ rings (Table 4).

The diagrams of the frontier molecular orbitals HOMO and LUMO, for three phenanthroline derivatives were shown in Fig. 3.

Fig. 4 illustrates the Tauc plot analysis of the studied compounds 1–3 in solution were presented in Fig. 4. The band gap values were evaluated through extrapolation by withdrawing straight line the linear trend observed in the spectral dependence of $(\alpha hc/\lambda)^{1/2}$ over a limited range of photon energies hc/λ [67].

3.4. UV-spectral analysis "Electronic transitions"

The UV–Vis spectra of the three phenanthrolines derivatives were calculated with TD-DFT approach (time-dependent density functional theory) at B3LYP/6-31G (d, p) level using methanol as solvent, including the Polarizable Continuum Model (PCM). The calculated absorption wavelength (λ), excitation energies, spectral assignments, oscillator strength (f), and major contributions are given in Table 5.

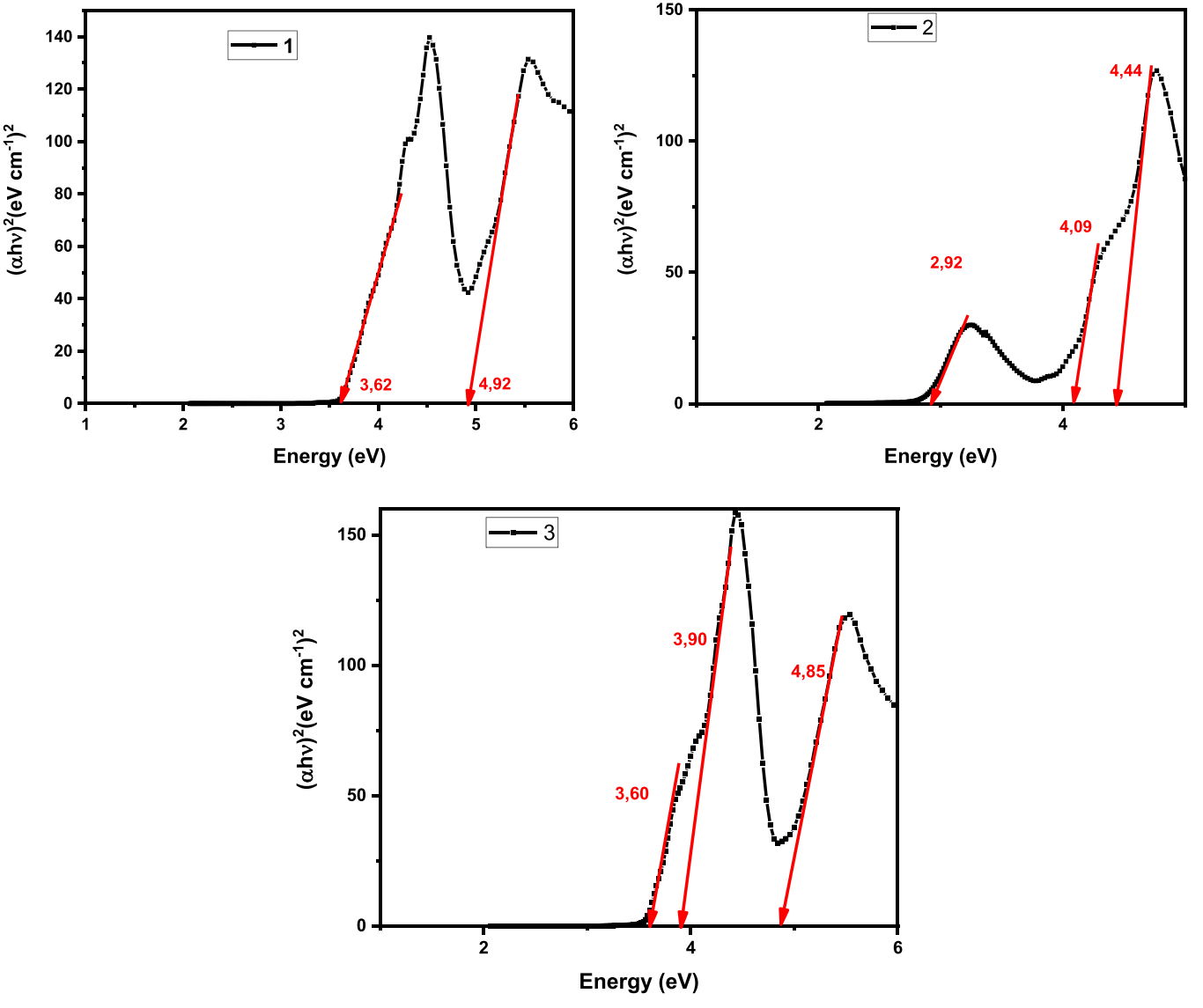

Fig. 4. Tauc Plot from UV–Vis analysis of the three studied compounds.

Table 5
The UV–vis Excitation energy (ΔE) and oscillator strength (f) for the three compounds C1, C2 and C3.

States	TD-DFT/6-31G (p, d) Methanol						Major Contributions (%)
	λ (nm)cal	ΔE	f	λ (nm)expt	CI coeff	Assignments	
C1							
S1	274	4.525	0.7125	274	0.67295	$n \rightarrow \pi^*$	H→ L (90.57)
S2	263	4.711	0.0025		0.42106		H-3 →L+2 (35.45)
S3	261	4.7363	0.0040		0.47219		H-3 →L+1 (44.59)
S4	257	4.809	0.4260		0.5246		H→L+1 (55.04)
S5	242	5.107	0.1268		0.44725		H→ *L* +2 (40.0)
S6	238	5.195	0.0332		0.45333		H-2→L (41,10)
S7	236	5.242	0.0019		0.39202		H-3 →L+1 (30.73)
S8	233	5.312	0.4685	224	0.37325	$\pi \rightarrow \pi^*$	H→ *L* +2 (43.89)
S9	226	5.464	0.0110		0.47692		H-5 →L+1 (45.49)
S10	224	5.520	0.2784		0.40001		H-1 →L (32.00)
C2							
S1	342	3.993	1.0286	384	0.65740	$\pi \rightarrow \pi^*$	H→ L (86.43)
S3	295	4.200	0.0101		0.59590		H→L+1 (71.01)
S4	278	4.4482	0.0374		0.53541		H→L+2 (57.33)
S6	269	4.6043	0.0079		0.48230		H-5→L (46.52)
S8	254	4.8797	0.0071		0.47608		H-2→L+2 (45,33)
S9	253	4.8906	0.1316		0.54840		H-1→L (60.14)
S10	248	4.9949	0.5888	262	0.56764		H-1→L+1 (64.44)
C3							
S1	311	3.9802	0.3381	280	0.64418	$n \rightarrow \pi^*$	H→ L (82.99)
S2	297	4.1744	0.4416		0.64176		H→L+2 (82.37)
S3	273	4.5403	0.5549		0.63437		H→L+2 (80.48)
S6	250	4.9438	0.3090		0.44322		H-1→L (39.28)
S7	248	4.9882	0.3688		0.44170		H→L+3 (39.01)
S8	243	5.1016	0.3116	226	0.56132		H-1→L+1 (63.01)

For phenanthrolines derivatives **1**, it can be seen that the transitions occur at 233 and 274 nm with transitions of H→L+2 (43.89%) and H→ L (90.57%) and experimental values of 224 and 274 nm. For phenanthrolines derivatives **3**, the wavelength of the absorption is observed at 243 and 311 nm with experimental values of 226 and 280 nm. The absorption band configurations are H-1→L+1 (63.01%) and H→ L (82.99%) respectively. For compound **2**, the transitions occur at 248 and 342 nm with experimental values of 262 and 384 nm while the state configurations are H-1→L+1 (64.44%) and HL (86.43%). The density of the state (DOS) diagram was analyzed using GaussSum 2.5 and presented in Fig. 5.

Fig. 5 shows the bonding, non-bonding and anti-bonding nature of the interactions between two orbital. The Positive value of DOS shows a bonding interaction, negative value shows anti-bonding interactions and zero value corresponds to the non-bonding interactions [68].

- The actual percent contribution $(\text{configuration coefficient})^2 \times 2 \times 100\%$.

3.5. Molecular electrostatic potential (MESP)

Mapped electrostatic potential surfaces for the three phenanthrolines derivatives have been calculated at the B3LYP/6-31G (p, d) basis set for optimized geometry. The information in the MEP program is used in a variety of diverse classical and quantum chemical models. A molecular electrostatic potential is a useful tool used for identifying the sites of chemical reactivity of molecules [69–71].

The different colors potential signified the different values of electrostatic potential. The Red colors represent the regions of the most negative electrostatic potential is related to electrophilic attacks, and blue represents the regions of the most positive sites electrostatic potential are associated to nucleophilic reactivity. Greater regions of intermediary potential, yellow and green, represents smaller regions of extreme potential. The potential increases in the order: red <orange< yellow< green < blue. Molecular electrostatic potential surfaces of the investigated phenanthroline derivatives are illustrated in Fig. 6. According to Fig. 6, the negative regions are mostly localized on the oxygen (O) atoms of NO_2 and $–OCH_3$ groups, orange color indicates electrophilic attack sites. The nitrogen atoms for the three phenanthrolines derivatives are positive regions signs as blue color which favored site for nucleophile attack.

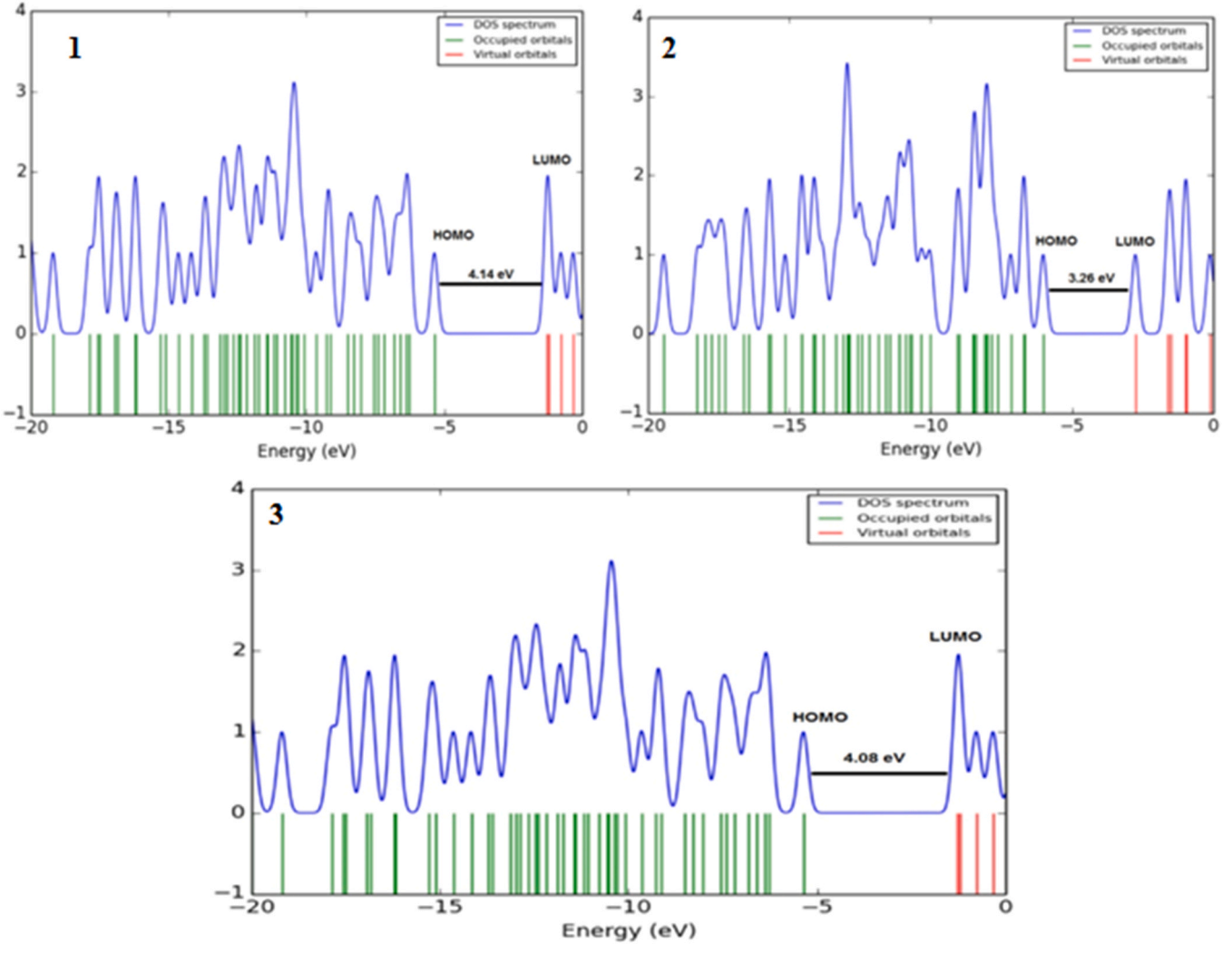

Fig. 5. Density of state of compound 1–3.

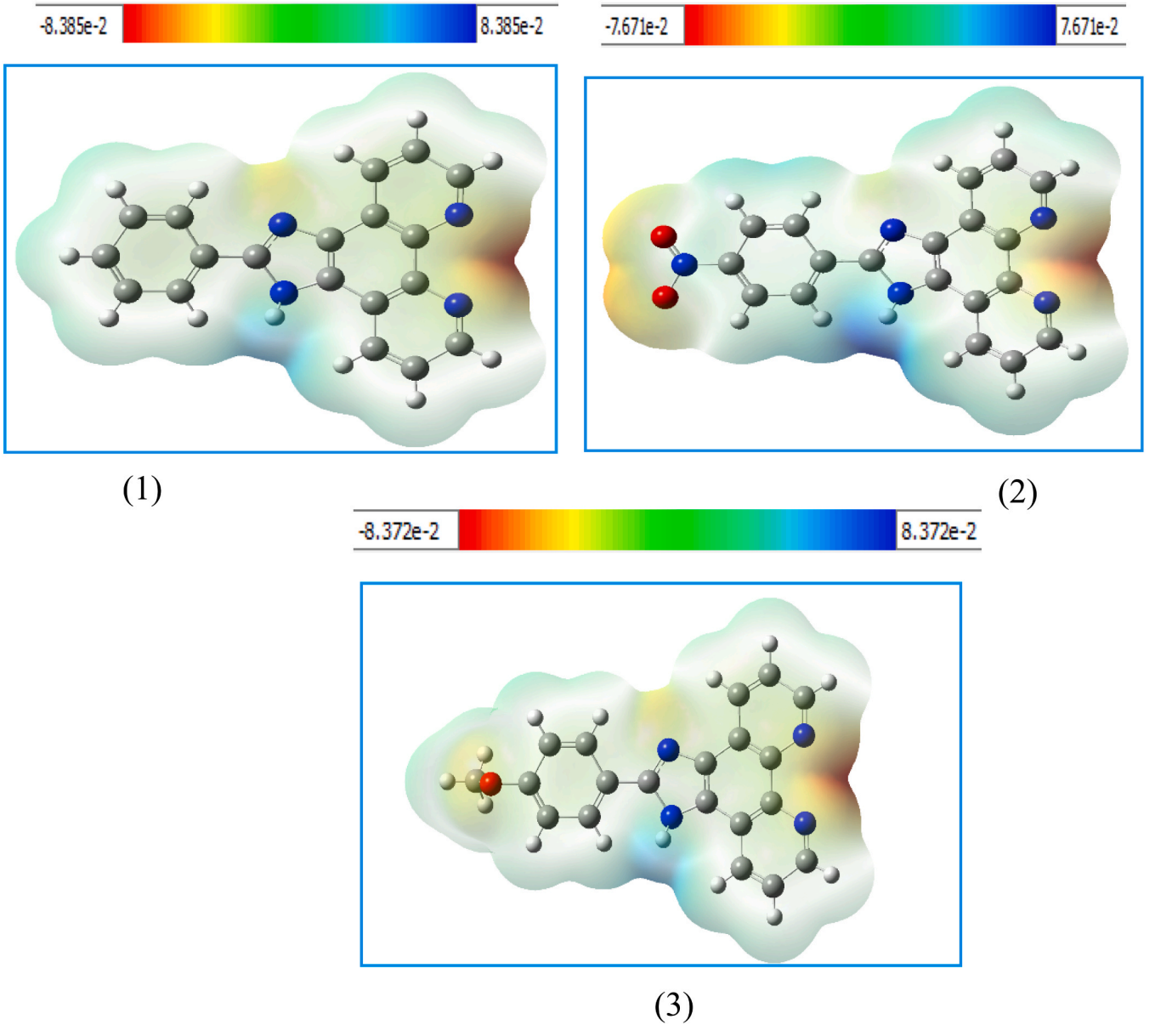

Fig. 6. Molecular electrostatic potential for compounds 1–3.

4. Conclusion

In summary, this investigation is based on three synthesized organic electronics phenanthroline derivatives, so we have presented here the synthesis, structural analysis, quantum chemical simulations and third-nonlinear optical (NLO) properties. The third-order non-linear response results expressed by $\chi^{<3>}_{THG}$susceptibility. Which was characterized and explored on thin films by using third-harmonic generation (THG) measurements at 1064 nm. We found that the third-nonlinear responses increase proportionally with the influence of the electron-donating groups NO2 > OCH3 > H. A few optical parameters like first hyperpolarizability, electronic transitions, frontier molecular orbital analysis and molecular electrostatic potential (MESP) are performed to evaluate the optical performance of designed phenanthrolines derivatives. Electron-donating groups modification on phenanthroline fragment causes narrowing of the HOMO-LUMO energy gap with blue-shifting in absorption maxima. The large dipole moment is noted in the three electronics phenanthroline derivatives designed**.** The experimental nonlinearity expressed by the third-order NLO properties susceptibility for the three phenanthrolines derivatives are in good agreement with theoretical results. Based on the obtained results we can conclude that the synthesized phenanthroline derivatives compounds are suitable candidates for NLO applications and father investigation on the modulation and the control of NLO response versus light polarizations and also versus diverse external stimulus is the subject for future diagnostic and studies.

Declaration of Competing Interest

We state that, the work described in this manuscript is the original experimental work performed by ourselves and was not published earlier in any other journal or submitted for consideration simultaneously. We request you to accept the manuscript for publication in Journal of Optik and looking forward to the pleasure of hearing from you soon.

References

[1] B. Kouissa, K. Bouchouit, S. Abed, Z. Essaidi, B. Derkowska, B. Sahraoui, Investigation study on the nonlinear optical properties of natural dyes: chlorophyll *a* and *b*, Opt. Commun. 293 (2013) 75–79.
[2] S. Arroudj, A. Aamoum, L. Messaadia, A. Bouraiou, S. Bouacida, K. Bouchouit, B. Sahraoui, Effect of the complexation on the NLO electronic contribution in film based conjugated quinoline ligand, Physica B 516 (2017) 1–6.
[3] S. Pramodini, P. Poornesh, Effect of conjugation length on non-linear optical parameters of anthraquinone dyes investigated using He–Ne laser operating in CW mode, Opt. Laser Technol. 62 (2014) 12–19.
[4] B. Kulyk, D. Guichaoua, A. Ayadi, A. El-Ghayoury, B. Sahraoui, Metal-induced efficient enhancement of nonlinear optical response in conjugated azo-based iminopyridine complexes, Org. Electron. 36 (2016) 1–6.
[5] V. Figà, J. Luc, B. Kulyk, M. Baitoul, B. Sahraoui, Characterization and investigation of NLO properties of electrodeposited polythiophenes, J. Eur. Opt. Soc. Rap. Publ. 4 (2009) 09016.
[6] I. Fuks-Janczarek, J. Luc, B. Sahraoui, F. Dumur, P. Hudhomme, J. Berdowski, I.V. Kityk, Third-order nonlinear optical figure of merits for conjugated TTF-quinone molecules, J. Phys. Chem. B 109 (20) (2005) 10179–10183.
[7] N. Terkia-Derdra, R. Andreu, M. Sallé, E. Levillain, J. Orduna, J. Garín, E. Ortí, R. Viruela, R. Pou-Amérigo, B. Sahraoui, A. Gorgues, J.-F. Favard, A. Riou, pi conjugation across the tetrathiafulvalene core: synthesis of extended tetrathiafulvalene derivatives and theoretical analysis of their unusual electrochemical properties, Chemistry 6 (2000) 1199–1213.
[8] B. Kulyka, D. Guichaouaa, A. Ayadia, A. El-Ghayourya, B. Sahraouia, Functionalized azo-based iminopyridine rhenium complexes for nonlinear optical performance, Dyes Pigments 145 (2017) 256–262.
[9] A. Ayadi, A. Szukalski, A. El-Ghayoury, K. Haupa, N. Zouari, N. Myśliwiec, J, B. Sahraoui, TTF based donor-pi-acceptor dyads synthesized for NLO applications, Dyes Pigments 138 (2017) 255–266.
[10] A. Ayadi, A. Szukalski, A. El-Ghayoury, K. Haupa, N. Zouari, J. Myśliwiec, F. Kajzar, B. Kulyk, B. Sahraoui, TTF based donor-pi-acceptor dyads synthesized for NLO applications, Dyes Pigments 138 (2017) 255–266.
[11] T.C. Ralph, R.W. Boyd, Better computing with photons, Science 318 (2007) 1251–1252.
[12] H.S. Nalwa, S. Miyata, Nonlinear Optics of Organic Molecules and Polymers, CRC press, 1996.
[13] F. Kajzar, J.D. Swalen (Eds.), Organic Thin Films for Waveguiding Nonlinear Optics, Gordon and Breach, Amsterdam, 1996.
[14] R.W. Boyd, Nonlinear Optics, Academic Press, 2003.
[15] E.D. D'silva, G.K. Podagatlapalli, S.V. Rao, D.N. Rao, S.M. Dharmaprakash, New, high efficiency nonlinear optical chalcone co-crystal and structure–property relationship, Cryst. Growth Des. 11 (2011) 5362–5369.
[16] W. Wu, Y. Liu, D. Zhu, Pi-conjugated molecules with fused rings for organic field-effect transistors: design, synthesis and applications, Chem. Soc. Rev. 39 (2010) 1489–1502.
[17] A. Airinei, R. Tigoianu, R. Danac, C.M. Al Matarneh, D.L. Isac, Steady state and time resolved fluorescence studies of new indolizine derivatives with phenanthroline skeleton, J. Lumin. 199 (2018) 2–12.
[18] C. Sall, A.-D. Yapi, N. Desbois, S. Chevalley, J.-M. Chezal, K. Tan, J.-C. Teulade, A. Valentin, Y. Blache, Design, synthesis, and biological activities of conformationally restricted analogs of primaquine with a 1,10-phenanthroline framework, Bioorg. Med. Chem. Lett. 18 (2008) 4666–4669.
[19] M.C. Nielsen, A.F. Larsen, F.H. Abdikadir, T. Ulven, Phenanthroline-2,9-bistriazoles as selective G-quadruplex ligands, Eur. J. Med. Chem. 72 (2014) 119–126.
[20] D. Wesselinova, M. Neykov, N. Kaloyanov, R. Toshkova, G. Dimitrov, Antitumour activity of novel 1,10-phenanthroline and 5-amino-1,10-phenanthroline derivatives, Eur. J. Med. Chem. 44 (2009) 2720–2723.
[21] (a) S. Thomas, G. Ruiz, G. Ferraudi, Preparation and reactivityof pendent CO2RhIII(phthalocyanine) bound to a poly(acrylate) backbone. Effects of the hypercoiled backbone on the association, photochemical, and thermal redox reactions of the pendent macrocycle, Macromolecules 39 (19) (2006) 6615–6621.
[22] T. Maldona-do, G. Ferraudi, G. Lappin, F. Godoy, Kinetic and mechanistic observations on the photoinduced isomerization reaction of organo-metallic chalcones: a steady state and flash photolysis study, ChemPhotoChem 2 (2) (2018) 95–104.
[23] J. Luc, K. Bouchouit, R. Czaplicki, J.-L. Fillaut, B. Sahraoui, Study of surface relief gratings on azo organometallic films in picosecond regime, Opt. Express 16 (2008) 15633–15639.
[24] J. Jayabharathi, V. Thanikachalam, M. Venkatesh, PerumalPhotophysical studies of fused phenanthrimidazole derivatives as versatile π-conjugated systems for potential NLO applications, Spectrochim. Acta A Mol. Biomol. Spectrosc. 92 (2012) 113–121.
[25] C.R. Moylan, R.D. Miller, R.J. Twieg, K.M. Betterton, V.Y. Lee, T.J. Matray, C. Nguyen, Synthesis and nonlinear optical properties of donor-acceptor substituted triaryl azole derivatives, Chem. Mater. 5 (1993) 1499–1508.
[26] M. Ammann, P. Bäuerle, Synthesis and electronic properties of series of oligothiophene-[1,10]phenanthrolines, Org. Biomol. Chem. 3 (2005) 4143–4152.

[27] G.S. Hong, Y.P. Zou, A.L. Antaris, S. Diao, D. Wu, K. Cheng, X.D. Zhang, C.X. Chen, B. Liu, Y.H. He, J.Z. Wu, J. Yuan, B. Zhang, Z.M. Tao, C. Fukunaga, H.J. Dai, Ultrafast fluorescence imaging in vivo with conjugated polymer fluorophores in the second near-infrared window, Nat. Commun. 5 (2014) 4206.
[28] A. Bencini, V. Lippolis, 1,10-Phenanthroline: a versatile building block for the construction ofligands for various purposes, Coord. Chem. Rev. 254 (17) (2010) 2096–2180.
[29] R.M. Ramadan, A.K. Abu Al-Nasr, O.A.M. Ali, Synthesis, spectroscopic, DFT studies and biological activity of some ruthenium carbonyl derivatives of bis-(salicylaldehyde)phenylenediimine Schiff base ligand, J. Mol. Struct. 1161 (2018) 100–107.
[30] A. Bencini, V. Lippolis, 1,10-Phenanthroline: a versatile building block for the construction of ligands for various purposes, Coord. Chem. Rev. 254 (2010) 2096–2180.
[31] M. Tamura, H. Ogata, Y. Ishida, Y. Takahashi, Design and synthesis of chiral 1,10-phenanthroline ligand, and application in palladium catalyzed asymmetric 1,4-addition reactions, Tetrahedron Lett. 58 (2017) 3808–3813.
[32] G. Conte, A. Bortoluzzi, H. Gallardo, [1,2,5]Thiadiazolo[3,4-f][1,10]phenanthroline as a building block for organic materials, Synthesis 2006 (2006) 3945–3947.
[33] A. Bencini, V. Lippolis, 1,10-Phenanthroline: a versatile building block for the construction of ligands for various purposes, Coord. Chem. Rev. 254 (2010) 2096–2180.
[34] G. Accorsi, A. Listorti, K. Yoosaf, N. Armaroli, 1,10-Phenanthrolines: versatile building blocks for luminescent molecules, materials and metal complexes, Chem. Soc. Rev. 38 (2009) 1690–1700.
[35] L. Viganor, O. Howe, P. McCarron, M. McCann, M. Devereux, The antibacterial activity of metal complexes containing 1,10-phenanthroline: potential as alternative therapeutics in the era of antibiotic resistance, Curr. Top. Med. Chem. 17 (2017) 1280–1302.
[36] Y. Xiong, X.H. Zou, J.Z. Wu, H.Y. Yang, L.N. Ji, Synth. React. Inorg. Met.-Org. Chem., 1998, pp. 1445–1454.
[37] T. Cardinaels, J. Ramaekers, P. Nockemann, K. Driesen, K.V. Hecke, L.V. Meervelt, S. Lei, S.D. Feyter, D. Guillon, B. Donnio, K. Binnemans, Imidazo[4,5-f]-1,10-phenanthrolines: versatile ligands for the design of metallomesogens, Chem. Mater. 20 (2008) 1278–1291.
[38] J. Wang, S. Xu, F. Zhao, H. Xia, Y. Wang, Computational and spectroscopic studies of the imidazole-fused phenanthroline derivatives containing phenyl, naphthyl, and anthryl groups, J. Mol. Struct. 1108 (2016) 46–53.
[39] J.Z. Wu, L. Li, T.X. Zeng, L.N. Ji, Effect of pyridine on the expression of cytochrome P450 isozymes in primary rat hepatocyte culture, Mol. Cell. Biochem. 173 (1997) 103–111.
[40] Q. Wang, H. Tamiaki, Highly efficient and selective turn-off quenching of ligand-sensitized luminescence from europium imidazo[4,5-f]-1,10-phenanthroline complex by fluoride ion, J. Photochem. Photobiol. A Chem. 206 (2009) 124–128.
[41] P. Lenaerts, A. Storms, J. Mullens, J. D'Haen, C. Görller-Walrand, K. Binnemans, K. Driesen, Thin films of highly luminescent lanthanide complexes covalently linked to an organic−inorganic hybrid material via 2-substituted imidazo[4,5-f]-1,10-phenanthroline groups, Chem. Mater. 17 (2005) 5194–5201.
[42] C. Hiort, P. Lincoln, B. Norden, DNA binding of.DELTA.- and.LAMBDA.-[Ru(phen)2DPPZ]2+, J. Am. Chem. Soc. 115 (1993) 3448–3454.
[43] K. Bouchouit, Z. Essaidi, S. Abed, A. Migalska-Zalas, B. Derkowska, N. Benalicherif, M. Mihaly, A. Meghea, B. Sahraoui, Experimental and theoretical studies of NLO properties of organic–inorganic materials base on p-nitroaniline, Chem. Phys. Lett. 455 (2008) 270–274.
[44] S. Arroudj, M. Bouchouit, K. Bouchouit, A. Bouraiou, L. Messaadia, B. Kulyk, V. Figa, S. Bouacida, Z. Sofani, S. Taboukhat, Synthesis, spectral, optical properties and theoretical calculations on schiff bases ligands containing o-tolidine, Opt. Mater. 56 (2016) 116–120.
[45] M. Bouchouit, Y. Elkouari, L. Messaadia, A. Bouraiou, S. Arroudj, S. Bouacida, S. Taboukhat, K. Bouchouit, Synthesis, spectral, theoretical calculations and optical properties performance of substituted-azobenzene dyes, Opt. Quant. Electron. 48 (2016) 178.
[46] K. Bouchouit, E. Bendeif, H.E. Ouazzani, S. Dahaoui, C. Lecomte, N. Benali-cherif, B. Sahraoui, Correlation between structural studiesand third order nlo properties of selected new quinolinium semi-organiccompounds, Chem. Phys. 375 (2010) 1–7.
[47] N. Zhen, Q. Yang, Q. Wu, X. Zhu, Y. Wang, F. Sun, W. Mei, Y. Yu, A novelly synthesized phenanthroline derivative is a promising DNA-damaging anticancer agent inhibiting G1/S checkpoint transition and inducing cell apoptosis in cancer cells, Cancer Chemother. Pharmacol. 77 (1) (2016) 169–180.
[48] J. Wang, S. Xu, F. Zhao, H. Xia, Y. Wang, Computational and spectroscopic studies of the imidazole-fused phenanthroline derivatives containing phenyl, naphthyl, and anthryl groups, J. Mol. Struct. 1108 (2016) 46–53.
[49] A. Patel, S.Y. Sharp, K. Hall, W. Lewis, M.F.G. Stevens, P. Workman, C.J. Moody, Fused imidazoles as potential chemical scaffolds for inhibition of heat shock protein 70 and induction of apoptosis. Synthesis and biological evaluation of phenanthro[9,10-d]imidazoles and imidazo[4,5-f][1,10]phenanthrolines, Org. Biomol. Chem. 14 (16) (2016) 3889–3905.
[50] H. Eshghi, M. Rahimizadeh, M. Hasanpour, M. Bakavoli, A novel imidazolium-based acidic ionic liquid as an efficient and reusable catalyst for the synthesis of 2-aryl-1H-phenanthro[9,10-d]imidazoles, Res. Chem. Intermed. 41 (7) (2015) 4187–4197.
[51] C. Yang, J. Luo, J. Ma, D. Zhu, L. Miao, Y. Zhang, L. Liang, M. Lu, Luminescent properties and CH_3COO^- recognition of europium complexes with different phenanthroline derivatives as second ligands, Synth. Metals 162 (2012) 1097–1106.
[52] D. Maker, R.W. Terhune, M.F. Niseno, C.M. Savage, Effects of dispersion and focusing on the production of optical harmonics, Phys. Rev. Lett. 8 (1962) 21–22.
[53] B. Sahraoui, J. Luc, A. Meghea, R. Czaplicki, J.L. Fillaut, A. Migalska-Zalas, Nonlinear optics and surface relief gratings in alkynyl–ruthenium complexes, J. Opt. A Pure Appl. Opt. 11 (2009), 024005.
[54] M.J. Frisch, G.W. Trucks, H.B. Schlegel, G.E. Scuseria, M.A. Robb, J.R. Cheeseman, G. Scalmani, V. Barone, B. Mennucci, G.A. Petersson, H. Nakatsuji, M. Caricato, X. Li, H.P. Hratchian, A.F. Izmaylov, J. Bloino, G. Zheng, J.L. Sonnenberg, M. Hada, M. Ehara, K. Toyota, R. Fukuda, J. Hasegawa, M. Ishida, T. Nakajima, Y. Honda, O. Kitao, H. Nakai, T. Vreven, J.A. Montgomery Jr., J.E. Peralta, F. Ogliaro, M. Bearpark, J.J. Heyd, E. Brothers, K.N. Kudin, V. N. Staroverov, T. Keith, R. Kobayashi, J. Normand, K. Raghavachari, A. Rendell, J.C. Burant, S.S. Iyengar, J. Tomas i, M. Cossi, N. Rega, J.M. Millam, M. Klene, J.E. Knox, J.B. Crossi, V. Bakken, C. Adamo, J. Jaramillo, R. Gomperts, R.E. Stratmann, O. Yazyev, A.J. Austin, R. Cammi, C. Pomelli, J.W. Ochterski, R. L. Martin, K. Morokuma, V.G. Zakrzewski, G.A. Voth, P. Salvador, J.J. Dannenberg, S. Dapprich, A.D. Daniels, O. Farkas, J.B. Foresman, J.V. Ortiz, J. Cioslowski, D.J. Fox, Gaussian 09, Revision C.01, Gaussian Inc., Wallingford CT, 2009.
[55] R. Dennington, T. Keith, J. Millam, GaussView Version 5.0.9, Semichem Inc. Shawnee Mission KS, 2009.
[56] A.D. Becke, Density-functional thermochemistry. III. The role of exact exchange, J. Chem. Phys. 98 (1993) 5648–5652.
[57] C. Lee, W. Yang, R.G. Parr, Development of the Colle-Salvetti correlation-energy formula into a functional of the electron density, Phys. Rev. B 37 (1988) 785–789.
[58] H. Lee, L. Xiong, Z. Gong, M. Ishitani, B. Stevenson, J.K. Zhu, The Arabidopsis HOS1 gene negatively regulates cold signal transduction and encodes a RING finger protein that displays cold-regulated nucleo–cytoplasmic partitioning, Genes Dev. 15 (5) (2001) 912–924.
[59] U. Gubler, C. Bosshard, Optical third-harmonic generation of fused silica in gas atmosphere: absolute value of the third-order nonlinear optical susceptibilityχ (3), Phys. Rev. B 61 (2000) 10702–10710.
[60] I. Fleming, Frontier Orbitals and Organic Chemical Reactions, John Wiley and Sons, New York, 1976, pp. 05–27.
[61] C.R. Zhang, H.S. Chen, G.H. Wang, Preparation and evaluation in vivo and in vitro of glimepiride gel-matrix controlled-release patch, Yao Xue Xue Bao 39 (2004) 640–644.
[62] Y. Sun, X. Chen, L. Sun, X. Guo, W. Lu, Nanoring structure and optical properties of Ga8As8, Chem. Phys. Lett. 381 (2003) 397–403.
[63] O. Christiansen, J. Gauss, J.F. Stanton, On-line study of growth kinetics of single hyphae of Aspergillus oryzae in a flow-through cell, Biotechnol. Bioeng. 63 (1999) 147–153.
[64] D.A. Kleinman, Nonlinear dielectric polarization in optical media, Phys. Rev. 126 (1962) 1977–1979.
[65] R. Mannhold, H. Kubinyi, H. Timmerman, Methods and Principles in Medicinal Chemistry, Volume 1, Wiley, 2000, p. 362.
[66] I. Fleming, Frontier Orbitals and Organic Chemical Reactions, John Wiley and Sons, New York, 1976, pp. 05–27.
[67] A. Zawadzka, K. Waszkowska, A. Karakas, P. Płóciennik, A. Korcala, K. Wiśniewski, M. Karakaya, B. Sahraoui, Diagnostic and control of linear and nonlinear optical effects in selected self-assembled metallophthalocyanine chlorides nanostructures, Dyes Pigments 157 (2018) 151–162.

[68] M. Chem, U.V. Waghmare, C.M. Friend, E. Kaxiras, A density functional study of clean and hydrogen covered a-MoO3(010): electronic structure and surface relaxation, J. Chem. Phys. 109 (1998) 6854–6860.
[69] J.S. Murray, K. Sen, Molecular Electrostatic Potentials, Concepts and Applications, Elsevier, Amsterdam, 1996.
[70] F.J. Luque, M. Orozco, P.K. Bhadane, S.R. Gadre, SCRF calculation of the effect of water on the topology of the topology of the molecular electrostatic potential, J. Phys. Chem. 97 (1993) 9380–9384.
[71] I. Sheikhshoaie, S.Y. Ebrahimipour, M. Sheikhshoaie, H.A. Rudbari, M. Khaleghi, G. Bruno, Combined experimental and theoretical studies on the X-ray crystal structure, FT-IR, ^{1}H NMR, ^{13}C NMR, UV-Vis spectra, NLO behavior and antimicrobial activity of 2-hydroxyacetophenone benzoylhydrazone, Spectrochim. Acta Part A Mol. Biomol. Spectrosc. 124 (2014) 548–555.